Modelling of mixing in a Taylor-Couette reactor with axial flow

Journal of Chemical Technology and Biotechnology **78** (2003), 227–235

Modelling of mixing in a Taylor-Couette Reactor with Axial Flow

Amjad Syed and Wolf-Gerrit Früh,
School of Engineering and Physical Sciences,
Heriot-Watt University, Edinburgh, UK

Abstract

Taylor-Couette flow with superimposed axial flow is becoming increasingly accepted as a novel reactor type offering a wide range of mixing regimes within a single reactor vessel, depending on the operating conditions of the reactor. To exploit the potential of such a reactor fully, the mixing processes in the reactor have to be well understood.

A variant of an established model to simulate flow in a Taylor-Couette reactor with axial flow is presented. The model, which is based on the description of the flow as a linked network of stirred tanks, attempts to develop a parameterisation of the mass exchange processes between Taylor vortices and the bypass stream on a rational basis. Some numerical results are presented and compared with results from the literature

Nomenclature

A	(m^2)	cross-sectional area of Taylor-Couette system
A^s	(m^2)	cross-sectional area of bypass stream
C	(kg/m^3)	tracer concentration
d	(m)	gap width of Taylor-Couette system
D	(m^2/s)	dispersion coefficient
D_s	(m^2/s)	axial dispersion coefficient
h	(m)	height of a vortex-bypass stage
k	(m/s)	vortex-bypass stream mass transfer coefficient
l	(m)	length scale to estimate gradient from difference
R	(m)	mean radius of Taylor-Couette system
R_i	(m)	radius inner cylinder of Taylor-Couette system
Re_θ		Rotational Reynolds number
Re_{ax}		Axial Reynolds number
S	(m^2)	Surface of vortex through which mass transfer occurs
Ta		Taylor number
$\overline{U}$	(m/s)	mean axial velocity, calculated from volume flow rate
U_v	(m/s)	drift velocity of the Taylor vortices
U_r	(m/s)	axial velocity in the bypass stream relative to the vortex
V	(m^3)	volume of a vortex-bypass stage
V_d		vortex drift velocity ratio
δ		vortex volume fraction
ν	(m^2/s)	kinematic viscosity
τ	(s)	Time for a vortex-bypass stage to drift by its height
Ω	(rad/s)	rotation rate of inner cylinder of Taylor-Couette system

Superscripts and subscripts

v	vortex
s	bypass stream
i	index of vortex-bypass stage

Version accepted for publication

1 Introduction

Taylor-Couette flow is a classical fluid dynamics phenomenon with the distinctive feature of a progression of clearly distinguishable flow regimes for different operating parameters — from laminar Couette flow via periodic Taylor vortices and chaotic flows to full turbulence [1]. A basic Taylor-Couette cylinder consists of a long cylinder co-axially mounted within an outer cylindrical shell, where the annular gap is filled with fluid as outlined in the vertical cross-section in Figure 1 (without the added pump). The system is forced by rotating either one or both of the cylindrical walls, although the outer cylinder is kept stationary in most applications. In addition to geometric parameters, the primary dynamic parameter is the Taylor number, which measures the relative contribution of the centrifugal force to viscous dissipation,

$$(1) \qquad Ta = \frac{d^3 R \Omega^2}{\nu^2},$$

where the d is the gap width, R the mean radius of the annulus (usually $d<<R$), ν the kinematic viscosity, and Ω the rotation rate of the inner cylinder. Some authors prefer a rotational Reynolds number,

$$(2) \qquad Re_\theta = \frac{dR_i \Omega}{\nu},$$

where R_i is the radius of the inner cylinder.

From a practical point of view, Taylor-Couette system has been employed in many applications such as chemical reactions and filtration processes. The recent idea of applying the Taylor-Couette system with axial flow to polymerisation or biochemical reactors[2,5] is being extensively studied for its mixing and dispersion characteristics. One obvious potential for its use in biotechnology is the fact that the agitation of the fluid and the resulting mixing arises primarily from a hydrodynamic instability which can provide good mixing without causing much mechanical damage to reactants or products. Furthermore, a judicious choice of the operating conditions provides a wide range of mixing regimes each of which may be exploited for different product specifications in the same reaction vessel.

Superimposing a net axial through-flow on the system (as indicated by the pump in Figure 1) adds another nondimensional dynamic parameter, the axial Reynolds number,

$$(3) \qquad Re_{ax} = \frac{d\overline{U}}{\nu},$$

where $\overline{U}$ is the average axial velocity as calculated from the volume flow rate and the cross-section of the annular gap. At small and moderate values of the axial Reynolds number, the general flow structure remains unaffected while the stack of vortices drifts at a velocity U_v through the annulus. This drift is usually measured by the vortex drift velocity ratio,

$$(4) \quad V_d = \frac{U_v}{\overline{U}},$$

which is a function of the Taylor number and axial Reynolds number.

When V_d is close to one, the vortices move in a stack and all axial mass transport is carried by the vortices. At relative drift velocities not equal to one, only some of the

axial mass transport is by the vortices. Mass balance then requires a by-pass stream winding around the vortices, which provides a route for fluid transport from the entry to the exit[6]. If V_d>1, the by-pass stream actually carries fluid back towards the entry region but if V_d<1, the by-pass stream enhances the downstream advection of material. Recently, Giordano et al. (1998) [3] observed an unusual behavior of slowing down of the displacement of the vortices with increase in the inner cylinder rotation, to an eventual flow type where the vortices were stationary.

The aim of this paper is to incorporate some mixing processes into a simple, well-established model of the Taylor-Couette system with an axial flow. The following section will introduce the mass transfer mechanisms thought to be active in the system and to derive a mathematical description of them which can be incorporated into the model presented by Giordano et al. (2000) [4, referred to as GGPC in the following] of the behaviour based on a stack of cells containing linked well-mixed sub-units representing the Taylor vortices and an axial flow stream respectively. The proposed expressions for the individual mass transfer terms are then incorporated into a numerical model. A description of some results and a rough comparison with results from GGPC [4] is presented in section 3.

2 The model

2.1 The mixing processes

It is commonly accepted to model the flow in a Taylor-Couette reactor as a stack of connected stirred tanks, e.g. [2,4]. Figure 2 describes the schematic concept of the flow found in a Taylor-Couette reactor with axial flow, where Figure 2(a) is taken from GGPC [4], while Figure 2(b) represents the flow structures seen in a typical flow regime of propagating Taylor vortices. Figure 2(c) is the model abstraction of the observations sketched in Figure 2(b). Figures 2(a) and (b) have in common that the flow is divided into distinct, perfectly mixed regions which represent vortices and the axial flow (by-pass region) where the by-pass region is subdivided into segments of the same axial length as the vortices. For the purpose of simplicity in this paper, the volumes of the vortex and the bypass stream do not change along the axial direction and each stage of height h is occupied by a vortex of volume fraction δ and a bypass segment of volume fraction $1-\delta$. Since the frame of reference is that of the drifting vortex, the axial flow may have a relative velocity upwards or downwards to this frame of reference. In addition, the drift of the vortices has to be represented in the model as a segment entering the system at the bottom while the final segment at the top leaves the system.

The model incorporates advection and dispersion effects along the by-pass stream, and dispersion between the by-pass and the vortices, where the basis of the dispersion is the finite-difference equivalent of the concentration gradient. The rate of change of concentration is proportional to the concentration difference in the two participating cells divided by a length scale representing the distance over which the difference is active. The equation for the concentration in vortex i is

(5)

$$V^v \frac{dC_i^v}{dt} = k_1 S^{v,1} \frac{C_i^s - C_i^v}{l_1} + k_2 S^{v,2} \frac{C_{i-1}^s - 2C_i^v + C_{i+1}^s}{l_2} + k_3 S^{v,3} \frac{C_{i-2}^v - 2C_i^v + C_{i+2}^v}{l_3}$$

where the first term on the right hand side is the transfer between the vortex and the bypass-stream segment of the same stage. The second term is the mass transfer between the vortex and the bypass segments of the neighbouring stages, and the last term is the transfer between the vortex and the nearest vortices on the same side of the bypass stream.

The corresponding equation for the adjacent segment of the by-pass stream is

$$V^s \frac{dC_i^s}{dt} = A^s |U_r| \left(C^s_{i-sign(U_r)} - C_i^s \right) + D_s A^s \frac{C^s_{i-1} - 2C_i^s + C^s_{i+1}}{l_s} + k_1 S^{v,1} \frac{C_i^v - C_i^s}{l_1} + k_2 S^{v,2} \frac{C^v_{i-1} - 2C_i^s + C^v_{i+1}}{l_2} \quad (6)$$

where the first term on the right hand side is the advection of the concentration by the axial velocity relative to the vortex. If the relative flow in the bypass stream is positive, fluid from segment i with concentration C_i^s leaving that segment is replaced by fluid from segment i-1 with concentration $C_{i-1}{}^s$, but if V_d>1, the relative velocity is negative and fluid from segment i+1 with concentration $C_{i+1}{}^s$ enters the segment i from above. This is the reason for using the absolute value of the relative velocity for the magnitude of the influx and the sign of the relative velocity to determine from which segment the fluid enters the stage. The second term on the right hand side is the axial dispersion along the bypass stream, while the third and last term represent the mass transfer between the vortices of the same and adjacent stages, respectively.

The cells near the end of the stack follow similar equations, where those exchange terms are simply omitted if they involve cells with indices less than one or larger than the number of vortices. The drift of the vortex-bypass stream cells is incorporated by incrementing the index of each cell once they have moved the distance of one cell height. The bottom cell is then initialized with a uniform concentration of the inlet condition.

While this work is based on the model by Giordano et al. [4], the model shows some elements not contained in their model. To keep our initial model as simple as possible some components of their models are neglected for the time being, namely any chemical reactions and the growth or shrinkage of vortices along the cylinder. Neglecting these does not imply in any way that they are unimportant aspects of the flow found in Taylor-Couette reactors. It merely reflects a research strategy of investigating some of the processes in isolation before building up a more complete model. The components included in our model are the mass transfer routes from a vortex to units in other cell stages. Figure 2(b) illustrates the reasoning for the possibility of mass transfer between vortex i, for example, and vortices i-2 and i+2 as well between that vortex and the bypass stream sections at stage i-1 and i+1. Furthermore, we allow for a drift velocity ratio of V_d>1.

As can be appreciated from the literature, the size and strength of a vortex depends on the Taylor and Reynolds numbers. As a result, the volumes, V^v and V^s, the bypass stream cross-section, A^s, and the contact areas between a vortex and its communicating cells, $S^{v,1-3}$, not only depend on the apparatus dimensions but also on the Taylor and Reynolds numbers. At first sight it therefore appears that this present model with two different volumes, four different areas, four different length scales, and four different transfer coefficients for a single-species fluid is extremely cumbersome and liable to give any desired result by fitting the parameters arbitrarily

to data. In the following section, some arguments are given to reduce the number of parameters greatly.

2.2 Model description

It appears from [4] that Giordano et al. used a fixed cross-sectional area of the bypass stream, while the contact area between a vortex and its surrounding bypass stream segment seems to be the surface of a circular or ellipsoidal torus of the volume of the vortex. Referring to Figure 2(b), it appears unlikely that the entire surface of the vortex is actually in contact with the main stream and, in our case, we limit the surface area between vortex *i* and bypass segment *i* to half the toroidal surface of the vortex. While the other half of the vortex surface does contribute to the other transport routes in equal parts, a different limiting surface is chosen here. Since the transport to neighbouring stages involves crossing stage boundaries, possibly by some form of boundary layer transport, a fixed portion of an inter-stage boundary is chosen for the limiting area available for this transport mechanism. Somewhat arbitrarily a value of 10% of the cross-sectional area of the annular section was chosen. The cross-sectional area between adjacent bypass segments is taken as the horizontal section remaining after the volume of the vortex has been deducted from the annular section of height of the vortex-bypass stream stage. Since all mass transfer processes are ultimately based on the same physical principles, the parameters in our formulation have all the same dimension (L^2T^{-1}) rather than the distinction between an axial dispersion coefficient (L^2T^{-1}) and vortex-bypass mass transfer coefficients (LT^{-1}) used by GGPC [4]. The authors felt that using dispersion coefficients throughout might provide some more physical insight into the processes involved.

The length scales involved in equations (5) and (6) in conjunction with the concentration difference represent the concentration gradient causing the mass transfer. To obtain a physically meaningful representation, appropriate length scales have to be used. The length scale for the axial dispersion is the path length of the bypass stream between the centre of adjacent bypass-stream segments, which to a reasonable approximation can be taken as the circumference of a semicircle with diameter of the segment height, $\pi h/2$. The scale for the vortex-bypass transfer within the same segment is the distance between the centre of the vortex and the centre of the bypass stream, which is half the gap width, $d/2$. The distance between a vortex and the neighbouring bypass stream segment is the height of the stage, h, and the distance between two communicating vortices is two stages, $2h$.

All these different length scales, areas and volumes can be related to a single parameter, δ, describing the relative size of the vortex. Since velocity maps[6] show that a stage can be approximated by an annular section with a square cross-section of height and width d, the relative volume parameter can be measured as the ratio of the vortex diameter to the gap width. Using this, the different areas can be calculated as follows

$$
(7)\quad
\begin{cases}
V = 2\pi R\, d\, h \\
V^{v} = \delta V \\
V^{s} = (1-\delta) V \\
A = 2\pi R\, d \\
A^{s} = (1-\delta) A \\
S^{v,1} = 2\pi R \pi\, \delta\, d = \pi\, \delta\, A \\
S^{v,2} = S^{v,3} = 2\pi R \times 0.1 d = 0.1 A \\
h = d \\
l_s = \frac{1}{2}\pi\, d \\
l_1 = \frac{1}{2} d \\
l_2 = d \\
l_3 = 2d
\end{cases}
$$

In a final simplification of the model, it was decided to use a uniform dispersion coefficient for all processes involved. While there may be good reasons why the shear dispersion from a vortex core to the bypass stream may be different, there seems to be good intuitive reason that they might be closely related (for example by a constant factor) rather than independent parameters. Since the organisation of the flow into the vortices and the bypass originates from hydrodynamic instabilities which tends to result in coherent structures of the same axial and radial size, it seems unlikely that the distribution of the velocity shear or the turbulence level can vary arbitrarily over the extent of the coherent flow structures. One might expect that the dispersion from the centre of the vortex outwards is slower than near the perimeter of the vortex for all flows, since the centre of the vortex is a region of small velocity shear while the outer region of the vortex is a region of high shear for all flows. If they are important at all, the mass transfer routes from a vortex to regions other than the adjacent bypass segment may follow a different *Re* and *Ta* dependency since these processes may involve transport through boundary layers rather than the Taylor vortex flow. However, as a starting point, all dispersion coefficients are taken as equal. A further study should then investigate the effect of a ratio of the vortex-bypass dispersion to the axial dispersion different from unity.

2.3 Model equations

Using (7) in (5) and (6) finally gives the equations for the model implementation.

$$
(8)\quad \frac{dC_i^{v}}{dt} = \frac{D}{d^2}\left[2\pi\left(C_i^{s} - C_i^{v}\right) + \frac{0.1}{\delta}\left(C_{i-1}^{s} - 2C_i^{v} + C_{i+1}^{s}\right) + \frac{0.1}{2\delta}\left(C_{i-2}^{v} - 2C_i^{v} + C_{i+2}^{v}\right)\right]
$$

and

$$
(9)\quad
\begin{aligned}
\frac{dC_i^{s}}{dt} = {} & \frac{|U_r|}{d}\left(C_{i-sign(U_r)}^{s} - C_i^{s}\right) \\
& + \frac{D}{d^2}\left[\frac{2}{\pi}\left(C_{i-1}^{s} - 2C_i^{s} + C_{i+1}^{s}\right) + \frac{2\pi\,\delta}{(1-\delta)}\left(C_i^{v} - C_i^{s}\right) + \frac{0.1}{2(1-\delta)}\left(C_{i-1}^{v} - 2C_i^{s} + C_{i+1}^{v}\right)\right].
\end{aligned}
$$

The equation for the respective concentrations in the first and last two stages follow equations (8) and (9) where simply the concentration differences involving non-existent stages were omitted. For example, the rate of change of concentration in vortex 1 reduced from (8) to

$$\frac{dC_1^v}{dt} = \frac{D}{d^2}\left[2\pi\left(C_1^s - C_1^v\right) + \frac{0.1}{\delta}\left(\quad - C_1^v + C_2^s\right) + \frac{0.1}{2\delta}\left(\quad - C_1^v + C_3^v\right)\right].$$

The equations were implemented in MATLAB, where two solvers, the nonstiff *ode45*-solver based on the Runge-Kutta method and the stiff *ode15s*-solver based on numerical differentiation formulae, were tested without appreciable difference. A relative tolerance of 10^{-9} was used to guarantee a good accuracy.

The drift of the vortices through the Taylor-Couette cylinder was modelled such that the index of a stage was incremented after the stages had travelled the height of a stage. The integration of the equation was interrupted after a time of $\tau = d\left(V_d\overline{U}\right)^{-1}$, the concentrations of one vortex-bypass stream segment was transferred to the next higher stage, the bottom stage was filled with a given inlet concentration (of zero in the present case), and the integration was restarted. The geometry and axial flow conditions were chosen to follow GGPC [4] as closely as possible, and they are summarised in table 1. Giordano et al. (1998) [3] report an injection location 90.4mm below the outlet and it is assumed that is was also used by them in GGPC. Assuming square stages, this corresponds to stage number 7 from the bottom out of 18 stages in the column, and all integrations were started with an initial concentration C_0 in vortex 7 only and zero concentrations everywhere else. Since all terms in the equations are proportional to a concentration difference, the actual value of C_0 does not affect the calculations besides a constant factor in all results. Starting with $C_0 = 1$ was used so that all results would give the concentration relative to the starting concentration in vortex 7.

3 Results

While the geometrical parameters were kept fixed in all integrations at values as close as possible to those of GGPC, a wide range of vortex drift velocity ratios, V_d, relative volume fractions, δ, and dispersion coefficients was investigated. It was found that the relative volume fraction usually had very little effect on the shape of the concentration curves, and only affected the magnitude of the scaling. A small volume fraction resulted in a small peak concentration at the outlet while a large volume fraction resulted in a large peak concentration. For this reason, only results for $\delta = 0.5$ are presented in the following. Figure 3 shows a synopsis of the results arranged such that each column represents a given value of the dispersion coefficient (indicated at the top of the column, ranging from $10^{-8}\mathrm{m}^2\mathrm{s}^{-1}$ to $10^{-3}\mathrm{m}^2\mathrm{s}^{-1}$) while the rows correspond to given values of the vortex drift ratio. The top row is for stationary vortices, $V_d = 0$, the penultimate row is for vortices moving at the average axial velocity, $V_d = 1$. The bottom row is for vortices moving slightly faster than the average axial velocity, which implies that the advection in the bypass stream moves fluid down to the next-lower stage. The intermediate values of $V_d = 0.76$ and $V_d = 0.94$, respectively, were chosen since GGPC presented experimental results at those values. The curves shown in all panels are the time traces of the concentration of the species at the outlet where the horizontal axis is the time in seconds after the release of the tracer in vortex 7, and the vertical axis is the concentration at the outlet

relative to the initial concentration in vortex 7. It should be noted that the scale of the concentration axis varies between the different graphs. All panels in the top rows and all panels on the third page are scaled with a maximum of C/C_0=0.05 while all remaining panels are scaled to C/C_0=0.5 on the first page and to C/C_0=0.2 on the second page, respectively. The outlet concentration was taken as the average of the concentration in vortex 18 and bypass segment 18, weighted by their volume fraction.

Comparing the first set of panels, for $D< 10^{-7}$, with the third set, $D>= 10^{-5}$, shows immediately that the vortex drift velocity ratio, V_d, has a very strong effect for slow dispersion but very little effect when the dispersion coefficient is relatively large. This is not surprising since the axial velocity, which is a direct function of the velocity ratio, carries most of the mass transfer if there is little dispersion, and its variation will have a large effect on the mass transfer. On the other hand, if the dispersion acts on a time scale faster than the mass transport by advection along the fluid column, the advection will be a secondary effect and will affect the mass transport much less.

It might be worth discussing the two singular cases first, namely V_d= 0 and V_d= 1. In the case of a stationary vortex, the flow effectively becomes that of a simple axial flow with stationary reservoirs of the tracer. At very small dispersion, the tracer content empties into the stream only very slowly and over a very long time, while the axial transport by advection is relatively fast. As the dispersion increases, the tracer moves into the axial stream much faster, resulting in a more pronounced, and earlier, peak in the concentration. At fast enough dispersion, the vortex acts almost as an instantaneous point source releasing the tracer into the uniform stream which then suffers fast axial dispersion together with relatively fast advection. At very large values of D, the axial spreading is so fast, that the peak concentration reaches the outlet almost instantly, while the advection washes out the remaining concentration much slower.

When V_d= 1, the relative axial velocity in the bypass stream is zero, and no advection takes place at all. All mass transport occurs through the gradual drift of the stages through the system and the dispersion. At very slow dispersion, most of the tracer remains in the initial vortex and its adjacent bypass stream segment, resulting in the very sharp peak after the time of travel of the stage from position 7 to position 18. At larger values of the dispersion coefficient, the spreading by dispersion becomes more and more pronounced relative to the shifting of the stage to the outlet.

At very strong dispersion, the difference between a stationary vortex and a co-drifting vortex is very small, since both release the majority of the tracer concentration into the axial stream, either by being part of the axial stream, or by quickly flooding the adjacent bypass stream segment which then spreads to the entire fluid column. At very slow dispersion, these two cases are very different. A stationary vortex acts like a continuous source which is gradually depleted, while the co-moving vortex acts like an instantaneous release of a fixed amount of tracer which then moves downstream and gradually spreads out. Intermediate velocity ratios show a mixture of these two extremes. When the vortices move slightly faster than at the average velocity, the upstream advection inhibits forward dispersion, and the concentration rises sharply to the maximum and then decays somewhat slower.

4 Discussion and summary

A model based on the concept of linked stirred tanks to represent the flow in a Taylor-Couette reactor with axial was developed. Unlike existing models, an attempt was made to capture the main behaviour through geometric constraints and flow

conditions while keeping the mass transfer coefficients to a minimum – a single value in this case. While no direct, and quantitative, comparison with experimental data and other models was possible in the time scale available, the model could capture the essential features of the observed dispersion behaviour reported in the literature.

Comparing this model to observations reported in GGPC, it seems that the relative sizes of the axial dispersion coefficient and the vortex-bypass mass transfer coefficient varied greatly. The change characterized by a change in the vortex drift velocity ratio from 0.76 (figures 5,6,7) to 0.94 (figure 8a) forced GGPC to drop the vortex-bypass mass transfer from three times the axial dispersion coefficient to half that value, while the present model (with some reservation) showed the observed tightening of the curve without any change in the dispersion coefficient. A careful look at their figure 8a, raises the question whether the velocity ratio is really less than unity. Even allowing for their more complex model, incorporating the variation of the vortex size with position cannot give an easy answer as to why the axial dispersion downstream is inhibited – something which would suggest an upstream advection caused by $V_d>1$. Having been forced to make the vortex-bypass mass transfer coefficient smaller than the axial dispersion coefficient when increasing the Taylor number, they then have to make it twenty times larger than the dispersion coefficient, while our model can reproduce that behaviour with a single value of D. That this value at $10^{-8}m^2/s$ is so much larger than the other range of $10^{-3}m^2/s$ is not surprising since one set of results are from the laminar regime, where the velocity shear is the dominant dispersive process while the last case is in the turbulent regime where one would expect a dispersion coefficient several orders of magnitudes larger than in a laminar regime.

The model presented in this paper, however, is still in its infancy and it would be preposterous to make any outrageous claims without further testing of the model. While the most important next stage should be to gather more experimental evidence on the dependence of the mixing behavior as a function of *Ta* and *Re*, the model itself must be tested in a variety of ways. Initially, the importance of the long-range dispersion should be tested. Are those additional terms really necessary? Secondly, the effect on allowing different (but closely related) values for the axial dispersion and the vortex-bypass exchange has to be investigated. After this, the features present in GGPC's model but not in ours must be incorporated to enable a proper comparison of the different models.

References:

[1] C. D. Andereck and S. S. Liu and H. L. Swinney (1986). Flow regimes in a circular Couette system with independently rotating cylinders. *J. Fluid Mech.* **164**, 155–183.

[2] G. Desmet, H. Verelst and G.V. Baron (1996). Local and global dispersion effects in Couette-Taylor flow-I. Description and modeling of the dispersion effects. *Chemical Engineering Science*, **51**, 1287-1298, and: Local and global dispersion effects in Couette-Taylor flow-II. Quantitative measurements and discussion of the reactor performance. *Chemical Engineering Science*, **51**, 1299-1309.

[3] R.C. Giordano, R.L.C. Giordano, D.M.F. Prazeres and C.L. Cooney (1998). Analysis of a Taylor-Poiseuille vortex flow reactor-I: Flow patterns and mass transfer characteristics. *Chemical Engineering Science,* **53**, 3635-3652.

[4] R.C. Giordano, R.L.C. Giordano, D.M.F. Prazeres and C.L. Cooney (2000). Analysis of a Taylor-Poiseuille vortex flow reactor-II: reactor modeling and performance assessment using glucose-fructose isomerization as test reaction *Chemical Engineering Science*, **55**, 3611-3626.

[5] K. Kataoka, H. Doi, T. Komai and M. Fitagarva (1975). Ideal plug flow properties of Taylor vortex flow. *Journal of Chemical Engineering Japan*, **8**, 472-476.

[6] S.T. Wereley and R.M. Lueptow (1999). Velocity field for Taylor-Couette flow with *an axial flow. Physics of Fluids,* **11**, 3637-3649.

Table 1. Values of parameters used for model integrations.

Quantity	Symbol (units)	Value	Quantity	Symbol (units)	Value / Range
Gap width	d (m)	8.2×10^{-3}	Aspect ratio (# of stages)		18
average axial velocity	$\bar{U}$ (m s^{-1})	7.1×10^{-5}	drift velocity ratio	V_d	0 – 1.1
kinematic viscosity	ν (m^2 s^{-1})	8.2×10^{-7}	vortex volume fraction	δ	0.1 – 0.9
Re_{ax}	$\frac{\bar{U}d}{\nu}$	0.71	Dispersion coefficient	D (m^2 s^{-1})	10^{-12} – 10^{-4}

Table 2. Values of parameters determined by GGPC [4] and estimated from the survey of this study. (Δ*: axial dispersion coefficient, and* k*: vortex-bypass mass transfer coefficient from GGPC)*

GGPC figure	*Ta*	V_d	Δ (m^2/s)	k (m/s)	Estimated order of D (m^2/s)
5	14,100	0.76	5×10^{-7}	1.5×10^{-6}	10^{-8}
6	14,100	0.76	5×10^{-7}	1.5×10^{-6}	10^{-8}
7	27,900	0.76	8×10^{-7}	4.0×10^{-6}	10^{-8}
8a	37,400	0.94	1×10^{-6}	5.0×10^{-7}	10^{-8}
8b	6.5×10^{6}	0.0	5×10^{-5}	1.0×10^{-3}	10^{-3}

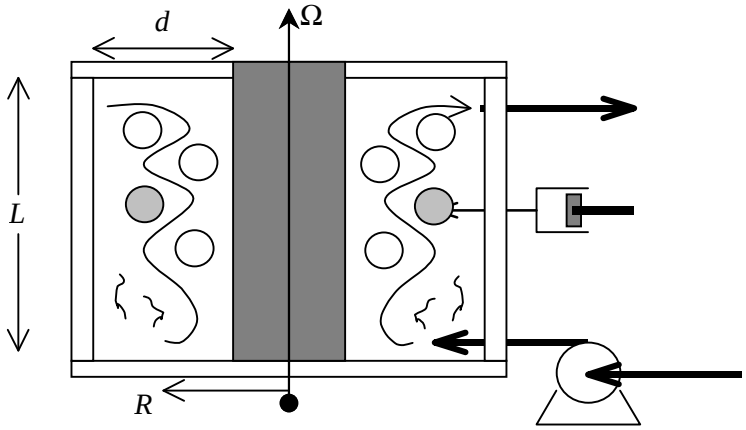

Figure 1. Cross-section through the Taylor-Couette cylinder. The dark inner cylinder rotates with rotation rate Ω while the remainder of the apparatus is stationary. The flow rate is provided by the shown pump and an injection port for adding tracer or a reactant is shown as a syringe.

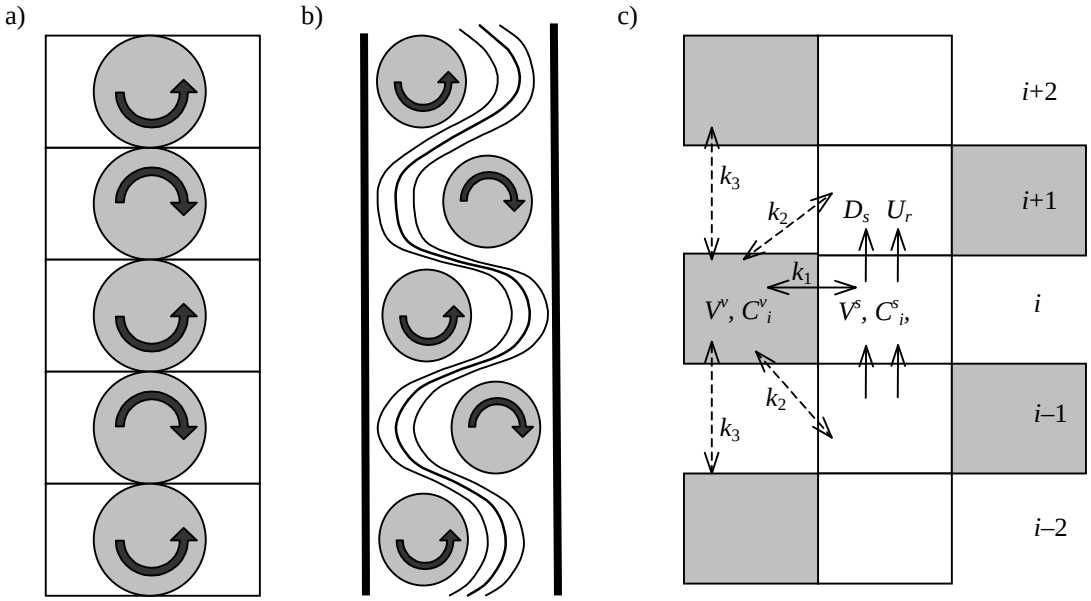

Figure 2. Schematic diagrams of the flow structures used to develop the mass balance models in (a) Giordano et al. (2000) [4] and (b) the present work. Figure (c) shows the subdivision of the different flow structures into well-mixed cells together with the different routes for mass transfer between the cells.

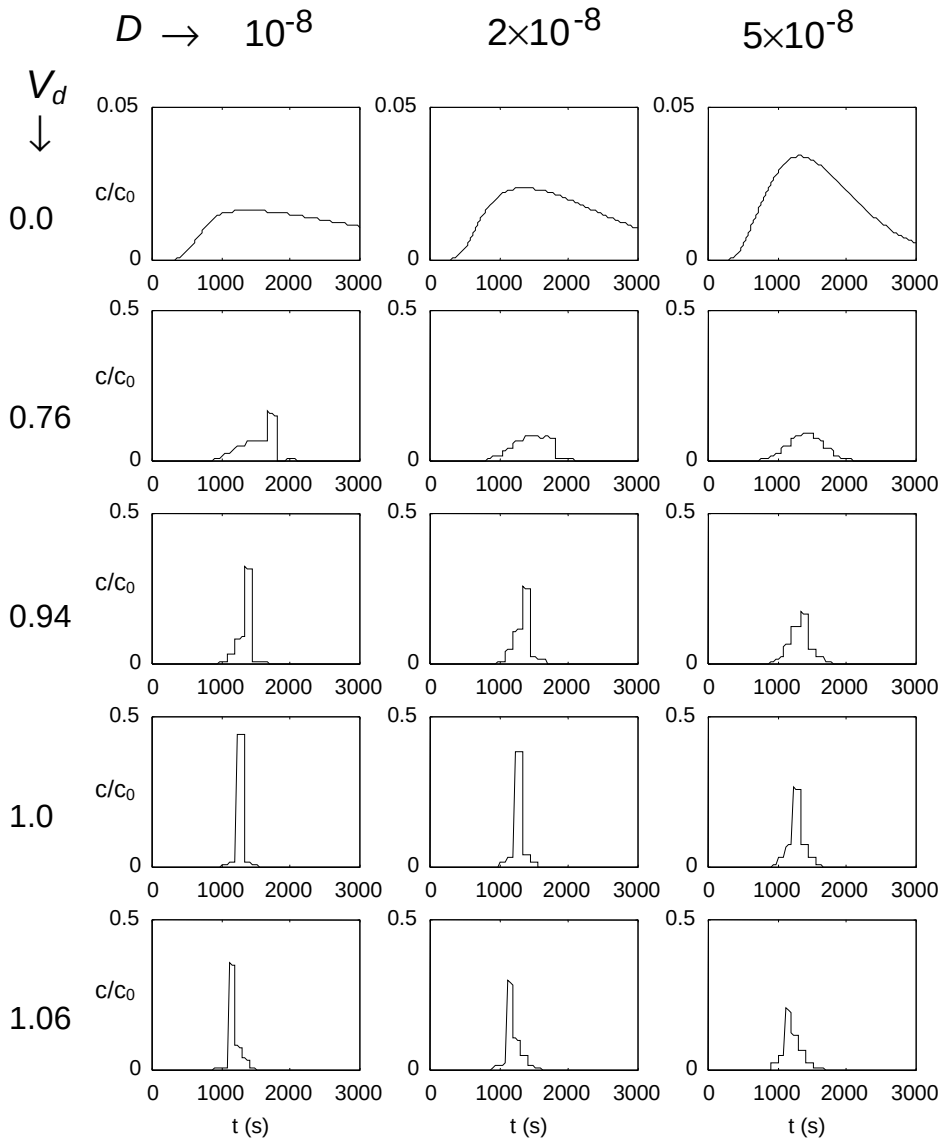

Figure 3. Relative tracer concentration at the outlet (stage 18) as a function of time, measured from the release of the concentration in the vortex in stage 7 for different values of the vortex drift velocity ratio, V_d*, and dispersion coefficient,* D *(m^2/s). This page shows results for weak dispersion,* $D<10^{-7}m^2s$*, the second page shows moderate dispersion, and the last page shows results for strong dispersion.*

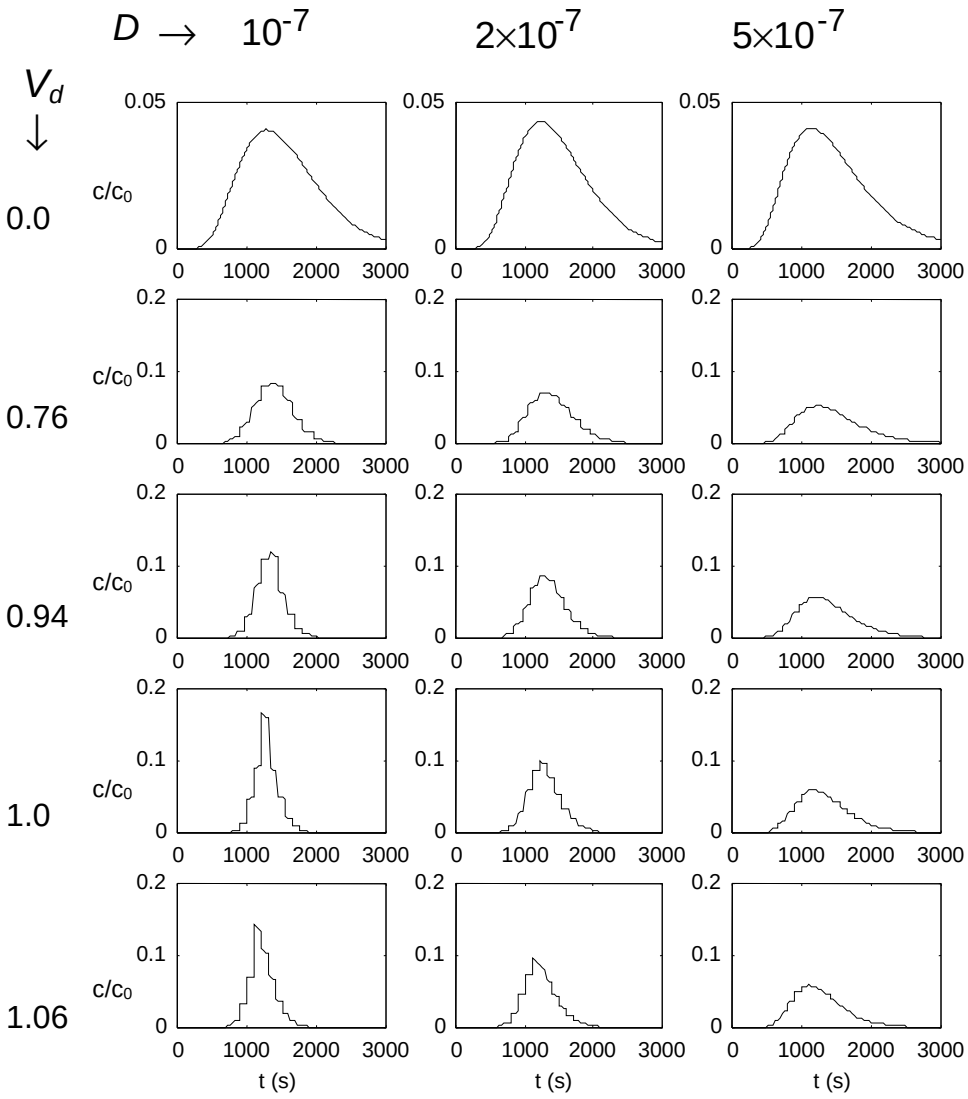

Figure 3 continued for moderate dispersion,$10^{-7}<=D<10^{-6}m^2s$.

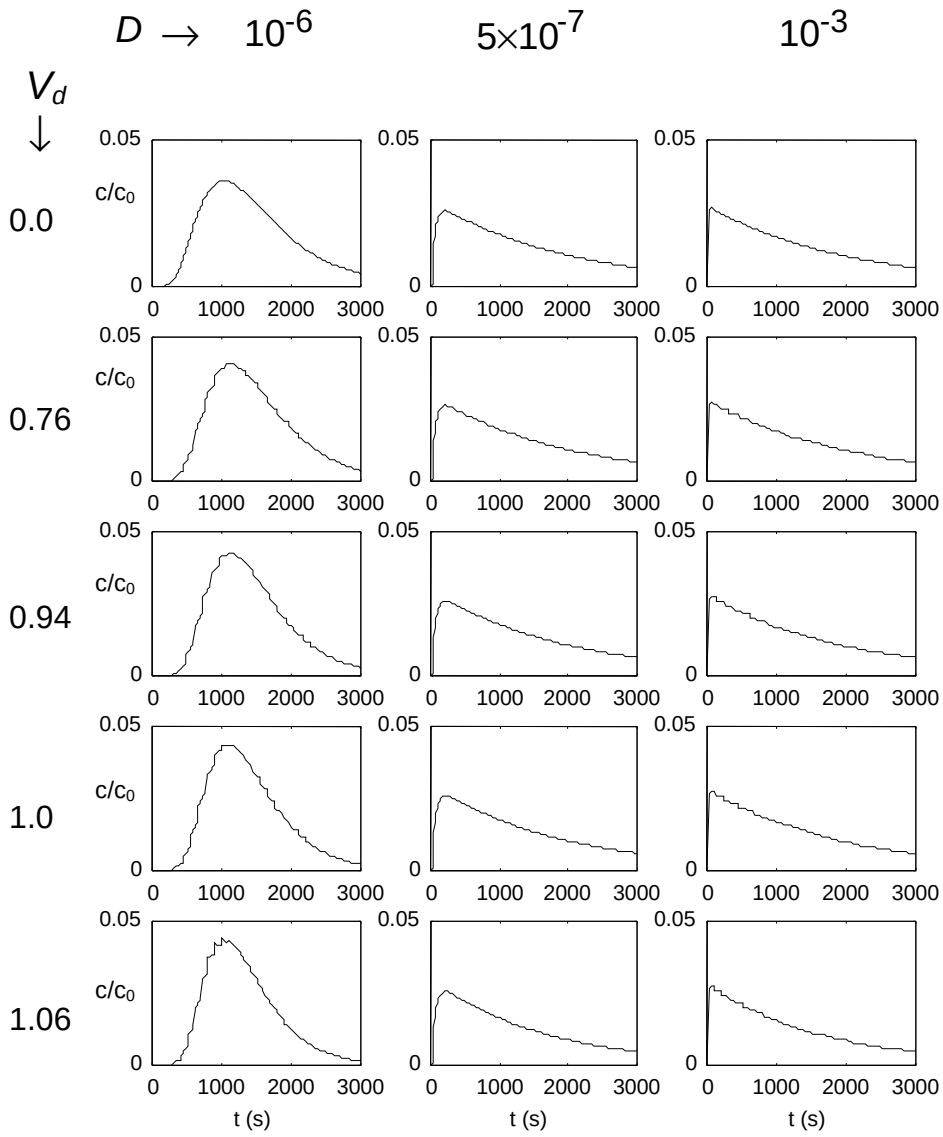

Figure 3 continued with final set of results for strong dispersion, D>=$10^{-6}$$m^2$s.